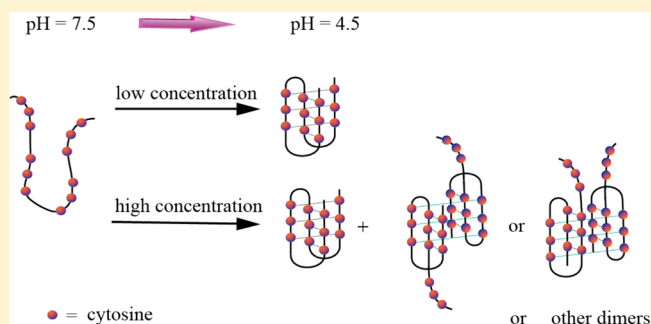


# pH-Induced Conformational Change and Dimerization of DNA Chains Investigated by Analytical Ultracentrifugation

Sha Wu,<sup>†</sup> Xiaoyan Wang,<sup>†</sup> Xiaodong Ye,<sup>\*,†</sup> and Guangzhao Zhang<sup>\*,‡</sup><sup>†</sup>Hefei National Laboratory for Physical Sciences at the Microscale, Department of Chemical Physics, University of Science and Technology of China, Hefei, Anhui 230026, China<sup>‡</sup>Faculty of Materials Science and Engineering, South China University of Technology, Guangzhou, People's Republic of China 510640

**ABSTRACT:** pH-induced conformational change of i-motif DNA has been studied by analytical ultracentrifugation. As pH increases, the hydrodynamic radius of individual DNA chains in aqueous solutions prepared by being heat-treated suddenly increases while the molar mass is constant, indicating that the conformation changes from an i-motif to a random coil. When DNA concentrations are higher than 1.0  $\mu\text{M}$ , relatively stable dimers are formed as pH sharply decreases from 7.5 to 4.5. Moreover, the weight percentage of the dimers increases with the initial DNA concentration. The study can help to understand the functions of the telomeres containing repeated cytosine-rich sequences and to develop DNA-based devices.



## INTRODUCTION

Since Gehring et al. reported a tetrameric DNA structure formed by  $d[\text{TC}_5]$  via cytosine and protonated cytosine base pairs ( $\text{C}\cdot\text{CH}^+$ ) on the basis of NMR spectroscopy, which was later confirmed by crystallographic study,<sup>1,2</sup> the cytosine-rich oligodeoxynucleotides and polynucleotides have attracted much attention in the past two decades. This is not only because of their biological relevance due to the identification of several nuclear proteins binding specifically to cytosine-rich strands<sup>3–8</sup> but also because of their role in the development of DNA-based devices.<sup>9–23</sup> Intramolecular i-motif structures at acidic pH were reported for several cytosine-rich sequences, for example,  $[\text{CCCCAA}]_4$  and  $[\text{CCTAA}]_3\text{CCC}$ .<sup>24–26</sup> With the help of several nuclear proteins recognized by Marsich and co-workers and Lacroix et al., i-motif structure might be stable at neutral pH and play an important role in gene expression regulation.<sup>4–6</sup> At  $\text{pH} > \sim 6.5$ , the cytosines are deprotonated and the conformation changes from an i-motif structure to a random coil. Thus, various DNA nanomachines have been constructed using the pH responsiveness of structures. For instance, Liu and Balasubramanian designed a DNA nanomachine which produces reversibly nanoscale motions on the basis of two strands of DNA, one of which can undergo pH-induced structural change.<sup>9</sup> Recently, other stimuli like UV light and electricity in noncontact mode were used to change the pH value and to control the conformation of DNA.<sup>15,27</sup> The pH-induced structural change of DNA has been studied by several techniques, including nuclear magnetic resonance (NMR),<sup>25</sup> fluorescence resonance energy transfer (FRET),<sup>12,28,29</sup> circular dichroism (CD),<sup>30,31</sup> UV–vis spectroscopy,<sup>28</sup> fluorescence correlation spectroscopy (FCS),<sup>29</sup> synchrotron small-angle X-

ray scattering (SSAXS) technique,<sup>32</sup> and quartz crystal microbalance with dissipation (QCM-D).<sup>33</sup> However, it is hard to observe the conformational change of individual DNA chains because most of the measurements were conducted at a relatively high concentration. Jin et al. used an SSAXS technique to study the pH-induced structural change of an oligonucleotide derivative  $[\text{H}_2\text{NC}_6\text{H}_{12}\text{-5}'\text{-CCC TAA CCC TAA CCC TAA CCC-3}'\text{-C}_6\text{H}_{12}(\text{CH}_2\text{OH})\text{NH}_2]$ .<sup>32</sup> Because the DNA concentration ( $C = 2.51 \pm 0.09 \text{ mg/mL}$ ) used is not low enough, monomers, dimers, and multimers might coexist.<sup>25</sup> Recently, Choi et al. used a combination of FRET and FCS to investigate the detailed conformation dynamics of DNA with a similar sequence of Alexa594- $\text{C}_{11}$ -5'-CCC TAA CCC TAA CCC TAA CCC-3'- $\text{C}_6$ -Alexa488. FCS is sensitive enough to detect the conformational change of DNA in aqueous solutions at a concentration of 1.0 nM, and so what they observed should be the individual chain behavior. Yet, the DNA has to be functionalized with extrinsic dyes as it is nonfluorescent. Considering that the weight average molar mass ( $M_w$ ) of the DNA is only several thousand, attachment of one or two dyes with  $M_w$  of several hundred should have nonignorable impact on the thermodynamics of the conformational change.<sup>28</sup> Possibly because of this reason, the diffusion coefficient was reported to decrease gradually with the increase in pH.<sup>29</sup> DNA chains often dimerize or form higher order aggregates, which has influence on their functions and properties of DNA related devices.<sup>34</sup>

Received: June 5, 2013

Revised: September 6, 2013

Published: September 6, 2013

To investigate the conformational change of individual DNA chains, a method with high sensitivity and resolution but without labeling DNA is needed. Analytical ultracentrifugation (AUC) is a good candidate for this purpose, as the hydrodynamic and thermodynamic parameters in solutions can be characterized with a relatively high resolution after the recent development in the data analysis software like SEDFIT program.<sup>35,36</sup> In this study, we have investigated the DNA behavior in aqueous solutions by use of AUC. Our study reveals that the hydrodynamic radius of individual DNA chains in aqueous solutions suddenly increases with pH, indicating that the change of conformation from an i-motif to a random coil is discontinuous. Relatively stable dimers can form as the pH changes from 7.5 to 4.5 when DNA concentrations are higher than 1.0  $\mu\text{M}$ . Moreover, our studies demonstrate that the DNA unimer with an intramolecular i-motif structure is more stable than the dimers at room temperature.

## EXPERIMENTAL SECTION

**Materials.** A 21-mer oligonucleotide and a control DNA with sequences of 5'-CCC TAA CCC TAA CCC TAA CCC-3' and 5'-TCT ATG CTG TTA CTC TGA CTC-3' from Sangon Biological Engineering (Shanghai) were purified by High Performance Liquid Chromatography (HPLC) prior to use.  $\text{Na}_2\text{HPO}_4 \cdot 12\text{H}_2\text{O}$  (99%) and  $\text{KH}_2\text{PO}_4$  (99.5%) from Sino-pharm were used as received. Ultrapure Milli-Q water with a resistivity of 18.2  $\text{M}\Omega \cdot \text{cm}$  used in all experiments was purified by filtration through a Millipore Gradient system after distillation. Phosphate-buffered saline (PBS) solutions with a constant ionic strength of 100 mM at different pH values were prepared by dissolving  $\text{Na}_2\text{HPO}_4 \cdot 12\text{H}_2\text{O}$  and  $\text{KH}_2\text{PO}_4$  in water.

**Sample Preparation.** DNA buffer solutions were prepared by four different procedures: (1) DNA was directly dissolved in PBS without further treatment. (2) DNA was first dissolved in  $\text{Na}_2\text{HPO}_4$  solution at pH 7.5, and then  $\text{KH}_2\text{PO}_4$  solution was introduced into the above DNA solutions under vortexing. All solutions prepared by this procedure have pH 4.5 and ionic strength of 100 mM but different DNA concentrations. (3) Instead of vortexing, the same volumes of DNA  $\text{Na}_2\text{HPO}_4$  solution and  $\text{KH}_2\text{PO}_4$  solution were mixed by using a Bio-Logic SFM300/S stopped-flow instrument to achieve efficient mixing. (4) All DNA solutions prepared by one of the above-mentioned three procedures were heated to 95  $^\circ\text{C}$  for 5 min and were cooled to room temperature over 2 h to form the desired structure.<sup>25,31,37,38</sup>

**Analytical Ultracentrifugation (AUC).** Sedimentation velocity (SV) experiments were conducted on a Proteomelab XL-A analytical ultracentrifuge (Beckman Coulter Instruments) at 20  $^\circ\text{C}$ , and the detector was UV-vis absorption optics with a wavelength range of 190–800 nm which could monitor the time-dependent radial concentration of DNA. A two-sector, charcoal-filled Epon centerpiece with quartz windows was used for all experiments. Four hundred microliters of DNA solution prepared by different procedures was added as the sample with 410  $\mu\text{L}$  of PBS as the reference. Three cells and a counterbalance were loaded into an An-60 Ti 4-hole rotor. Before the angular velocity increased to the final rotational speed of 60 000 rpm, DNA solution was thermostatted at 20  $^\circ\text{C}$  and at 0 rpm for at least 2 h. About 200 scans of data for every DNA solution were acquired at a time interval of 3 min at a wavelength range of 260–300 nm to ensure that the absorbance was lower than 1 to satisfy the Lambert–Beer

Law. Data were collected using the software provided with the instrument and were analyzed by using software SEDFIT.<sup>35</sup> The sedimentation and diffusion processes of molecules during centrifugation can be described by the Lamm equation

$$\frac{\partial c}{\partial t} = \frac{1}{r} \frac{\partial}{\partial r} \left[ r \cdot D \frac{\partial c}{\partial r} - \omega^2 r^2 s c \right] \quad (1)$$

where  $c$ ,  $r$ ,  $t$ ,  $\omega$ ,  $s$ , and  $D$  are the concentration of the solute, the radial distance from the axis of rotation, the sedimentation time, the angular velocity, the sedimentation coefficient, and the diffusion coefficient, respectively. The sedimentation coefficient is defined as  $s = u/\omega^2 r$  with the sedimentation velocity  $u$  of the solute. The continuous distribution  $c(s)$  implemented in SEDFIT was used to fit the absorbance profiles with the Lamm equation solutions using the maximum entropy regularization which followed the CONTIN method provided by Provencher.<sup>39,40</sup> The confidence level was set to  $p = 0.95$  in our study. Assuming that all species in solution have the same weight-average frictional ratio, because  $c(s)$  model in SEDFIT program could distinguish boundary spreading due to size heterogeneity from diffusion, molar mass and diffusion coefficient can be evaluated with a combination of the Svedberg equation and the Stokes–Einstein equation:

$$M = \frac{s \cdot k_B \cdot N_A \cdot T}{D \cdot (1 - \bar{v} \cdot \rho_s)} \quad (2)$$

$$D = \frac{k_B \cdot T}{f} = \frac{k_B \cdot T}{6\pi\eta R_h} \quad (3)$$

with molar mass  $M$ , the Boltzmann constant  $k_B$ , the Avogadro's number  $N_A$ , the absolute temperature  $T$ , the solvent density  $\rho_s$ , the partial specific volume of the solute  $\bar{v}$ , the frictional coefficient  $f$ , the solvent viscosity  $\eta$ , and the hydrodynamic radius  $R_h$ . The partial specific volume of DNA is 0.55  $\text{mL} \cdot \text{g}^{-1}$  according to Cohen and Eisenberg<sup>41</sup> and Durchschlag.<sup>42</sup>

## RESULTS AND DISCUSSION

The high-resolution sedimentation coefficient distribution can be achieved in one experiment via sedimentation velocity experiment with the help of SEDFIT program developed by Schuck.<sup>35,43</sup> We first investigated the effect of the preparation procedure on the structure of DNA. Figure 1 clearly shows that the DNA buffer solution with a directly dissolving procedure is

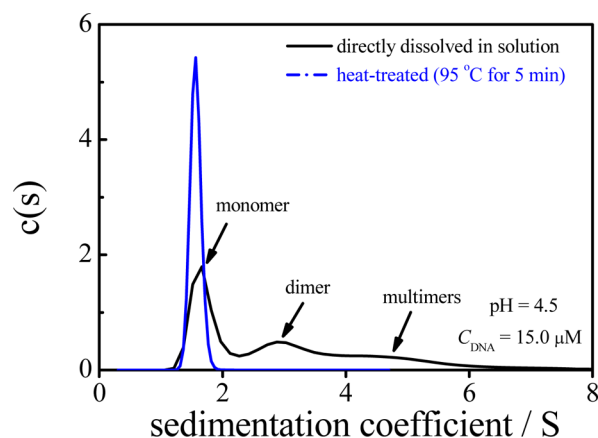


**Figure 1.** Sedimentation coefficient distribution of i-motif DNA with and without being heat-treated at pH 4.5 and  $T = 20$   $^\circ\text{C}$ .

heterogeneous with a concentration of  $15.0 \mu\text{M}$  at pH 4.5. Assuming that all species have a similar frictional ratio, the molar masses of the two main species are  $6.1 \times 10^3$  and  $1.32 \times 10^4$  g/mol, respectively, indicating that they are monomers and dimers. Then, another procedure was used to prepare DNA buffer solutions as we mentioned in Sample Preparation, that is, DNA solutions were heated to  $95^\circ\text{C}$  for 5 min and were cooled to room temperature over 2 h to form the desired structure. The same or similar procedures were used to obtain monomeric DNA i-motif.<sup>25,31,37,38</sup> Especially, only a single band corresponding to monomeric DNA at pH 5 with a DNA concentration of  $210 \mu\text{M}$  was reported by using native gel electrophoresis.<sup>38</sup> Actually, both the size and conformation of DNA can affect the migration rate of DNA in a gel; it is hard to draw a conclusion.

Figure 1 shows that only one species with a molar mass of 6090 g/mol exists, indicating that the species is monomeric DNA. As the temperature increases above the melting temperature of the DNA,<sup>37,44</sup> it adopts a random coil conformation. The increase in the flexibility of the DNA chain can help to find the most favorable structure with the lowest free energy during the cooling process, that is, the monomeric i-motif. Our studies also revealed that there was only one peak with a narrow distribution at pH 8.0 by DNA buffer solution procedures 1 and 4 (not shown). This is because all cytosines are unprotonated and because there are strong electrostatic repulsive forces between nucleotides in the same or different DNA chains.

**pH-Induced Conformational Change.** After eliminating the heterogeneity of the DNA solutions by heat treatment, we investigated the structural change of i-motif DNA in comparison with control DNA at different pH values. Figure 2 shows the sedimentation coefficient distribution of i-motif

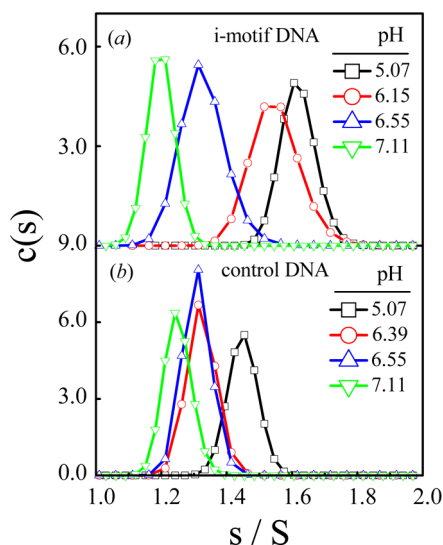


**Figure 2.** Sedimentation coefficient distribution of (a) i-motif DNA and (b) control DNA at four pH values, where the concentration of the DNA was kept at  $3.0 \mu\text{M}$ .

DNA and control DNA as a function of pH, where the DNA concentration is  $3.0 \mu\text{M}$ . As seen below, such a low concentration makes observation of the individual DNA chain behavior by AUC possible. As we know, DNA concentration was much higher in the previous SSAXS studies;<sup>32</sup> it is difficult to observe the conformational change of individual DNA

chains. On the other hand, labeling with extrinsic fluorophores might slightly change the structure of DNA at different pHs.<sup>29</sup> Alberti and Mergny reported that the attachment of fluorescein and rhodamine groups at both ends of the oligonucleotide with a sequence of  $d(\text{GGGTTA})_3\text{GGG}$  slightly changed the stability of the quadruplex.<sup>45</sup> Mergny also mentioned that the attachment of fluorescein or tetramethylrhodamine led to imperfect superimposition of the melting profiles measured by UV spectroscopy.<sup>28</sup> In the present study, the DNA behavior can be directly characterized by AUC without any labeling.

Figure 2 also shows that the samples have narrow distribution at different pH values. The sedimentation coefficient ( $s$ ) of either i-motif DNA or control DNA increases as pH decreases. This is because the effective charge increases with pH due to the unprotonation of cytosine or adenine. However, the change in  $s$  for i-motif DNA is larger than that for control DNA because of the additional conformational change of i-motif DNA.

Figure 3 shows the change in  $s$  of DNA as a function of pH. For i-motif DNA, at pH < 6,  $s$  slightly decreases as pH

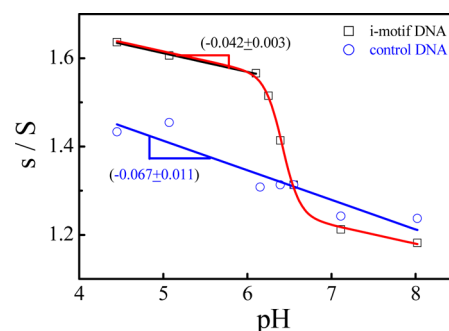


**Figure 3.** pH dependence of the sedimentation coefficient of i-motif DNA ( $\square$ ) and control DNA ( $\circ$ ), where the concentration of both DNA was kept at  $3.0 \mu\text{M}$ .

increases. At pH > 6,  $s$  decreases dramatically as pH increases to  $\sim 7$ , indicating the conformational change from an i-motif to a random coil in the range of pH 6–7 because of the unprotonation of the cytosine. Figure 3 shows that for i-motif DNA, the data can be fitted by a sigmoidal curve with a midpoint at pH  $\sim 6.4$ , which is in agreement with the results reported by Kaushik et al.<sup>37</sup> and Manzini et al.<sup>46</sup> Then,  $s$  slightly decreases as pH increases from 7 to 8. For control DNA,  $s$  slightly changes in the range of pH 4.5–8. Figure 3 also shows that the slope of the decrease in  $s$  of i-motif DNA in the range pH < 6 is similar to that of control DNA in the range  $4.5 < \text{pH} < 8$ , indicating that the reason for the change in  $s$  in these pH ranges is similar to what we mentioned previously, namely, the effective charge in DNA increases because of the unprotonation of cytosine or adenine.

Figure 4 shows the pH dependence of  $R_h$  and  $D$  for i-motif DNA and control DNA. At pH < 6,  $R_h$  is nearly a constant, indicating that the DNA adopts an i-motif conformation with a smaller  $R_h$  of  $\sim 1.33$  nm. The sudden increase in  $R_h$  in the range of pH 6–7 reflects the conformational change of DNA from an i-motif to a random coil. Then,  $R_h$  levels off at pH > 7. For control DNA, we only observed that  $R_h$  gradually increases with increasing pH. From Figure 4, we know that  $D$  of i-motif DNA at pH 5.07 is  $1.64 \times 10^{-10} \text{ m}^2 \cdot \text{s}^{-1}$ , slightly higher than the value  $D = 1.57 \times 10^{-10} \text{ m}^2 \cdot \text{s}^{-1}$  at similar pH 5.2 reported by Choi et al. and measured by FCS technique, possibly because of the



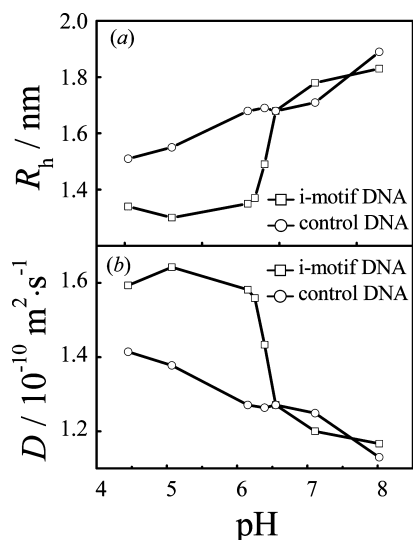


**Figure 4.** pH dependence of (a) the hydrodynamic radius ( $R_h$ ) and (b) the diffusion coefficient ( $D$ ) of i-motif DNA ( $\square$ ) and control DNA ( $\circ$ ), where the concentration of both DNA was kept at  $3.0 \mu\text{M}$ .

decrease in molar mass without labeling with extrinsic fluorophores. Furthermore,  $D$  decreases dramatically when pH is in the range of pH 6–7.<sup>29</sup> Choi et al. found that the diffusion coefficient of the i-motif DNA labeled with Alexa488 and Alexa594 at 3' and 5' ends gradually decreased with the increase in pH, further indicating the non-negligible influence of the extrinsic dyes on the dynamics of the i-motif DNA.<sup>28,29</sup> Both CD and UV-vis spectroscopy have been used to study the pH-induced conformational change of i-motif DNA. However, it is difficult to distinguish species with similar physical properties by these methods, as mentioned by Dailey et al.,<sup>47</sup> for example, these methods might not be able to distinguish whether a species is a folded monomer, dimer, or multimer.

Figure 5 shows the pH dependence of the molar mass ( $M_w$ ) of i-motif DNA and control DNA, where the DNA

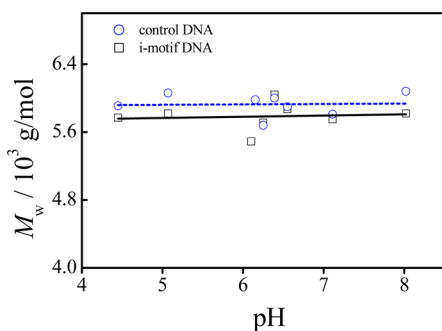


**Figure 5.** pH dependence of the molecular weight ( $M_w$ ) of i-motif DNA ( $\square$ ) and control DNA ( $\circ$ ), where the concentration of both DNA was kept at  $3.0 \mu\text{M}$ .

concentration was kept at  $3.0 \mu\text{M}$ . The molar masses of i-motif DNA and control DNA are nearly a constant at different pH values. The average measured  $M_w$  of i-motif and control DNA are  $5800 \text{ g/mol}$  and  $6000 \text{ g/mol}$ , respectively, close to the real values of monomeric DNA within the experimental errors, clearly indicating that we observed the intramolecular conformational change of individual DNA chains and that no dimers and multimers exist in our system. Jin et al. investigated

the structure of i-motif DNA with a similar sequence at different pH values by the use of SSAXS technique.<sup>32</sup> The pH-dependence of the radius of gyration can be calculated from the full scattering curve. However, probably because of the small molecular weight of DNA, a relatively high concentration ( $C = 2.51 \pm 0.09 \text{ mg/mL}$ ) was used during the study. Thus, monomers, dimers, and multimers might coexist in their system which may complicate the system.<sup>25</sup>

**Dimerization.** The DNA molecules can form dimers on certain conditions. Figure 6 shows the sedimentation coefficient

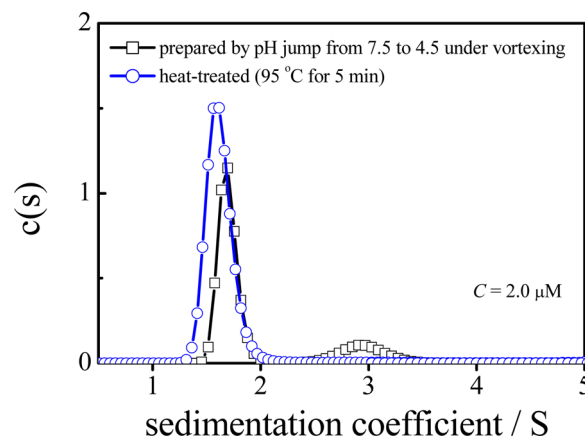


**Figure 6.** Sedimentation coefficient distribution of i-motif DNA prepared by being heat-treated ( $95 \text{ }^\circ\text{C}$  for 5 min) and by a pH-jump method under vortexing, where the final pH = 4.5 and the concentration of the DNA was kept at  $2.0 \mu\text{M}$ .

distribution of i-motif DNA prepared by being heat-treated and by a pH-jump method from pH 7.5 to 4.5 under vortexing. A new peak was observed with a sedimentation coefficient of  $2.87 \text{ S}$  corresponding to a molar mass of  $1.37 \times 10^4 \text{ g/mol}$ , indicating the formation of dimers. Each DNA starts to fold from a random coil to an i-motif after the pH suddenly changes from 7.5 to 4.5. During the folding process, intermediates collide with each other. Some of the collisions will lead to the formation of dimers if the relative orientation of the intermediates is right. We are able to estimate the mean collision time ( $t_c$ ) between two DNA chains in the buffer solution

$$t_c \sim \bar{x}^2 / 2D \quad (4)$$

where  $\bar{x}$  is the mean distance between two neighboring DNA chains which is related to the DNA concentration ( $2.0 \mu\text{M}$ ), and  $D$  is the average translational diffusion coefficient of DNA chains, which has been accurately measured by sedimentation velocity as shown in Figure 4. The value of estimated  $t_c$  is  $\sim 0.03 \text{ ms}$ . The stopped-flow circular dichroism measurements show that the folding process of i-motif DNA with the same sequence finishes in  $\sim 300 \text{ ms}$ ,<sup>31</sup> clearly indicating that only a very small portion of the collision is effective for the formation of dimers; otherwise, most of the DNA chains should form dimers. Moreover, Figure 6 shows that the weight percentage of the dimer obtained by integration of the sedimentation coefficient distribution is 18%.

The formation of dimers requires that two DNA single chains collide with each other, and no collision takes place before the completion of the folding of a single DNA chain if the DNA concentration is low enough. Furthermore, the frequency of collision will increase with the initial DNA

concentration. As a result, the weight percentage of the unimer concentration will decrease. Figure 7 shows that almost all of

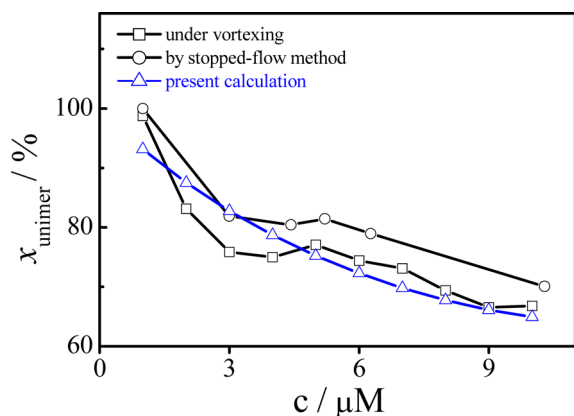
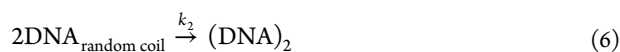


**Figure 7.** The initial concentration of i-motif DNA dependence of the weight percentage of the unimer ( $x_{\text{unimer}}$ ) prepared by vortexing ( $\square$ ) and by use of stopped-flow technique ( $\circ$ ), respectively, where  $T = 20$  °C. The present calculation of the  $x_{\text{unimer}}$  for  $k_1 = 8 \text{ s}^{-1}$  and  $k_2 = 6 \times 10^5 \text{ M}^{-1}\cdot\text{s}^{-1}$  is also plotted ( $\Delta$ ).

the DNA chains fold into an intramolecular i-motif structure with a DNA concentration of  $1.0 \mu\text{M}$  and that the weight percentage of the unimer ( $x_{\text{unimer}}$ ) decreases with DNA concentration from  $1.0 \mu\text{M}$  to  $10.0 \mu\text{M}$ . For the same DNA concentration,  $x_{\text{unimer}}$  prepared by use of the stopped-flow technique is a little bit larger than that prepared under vortexing, indicating that the method by stopped-flow technique is more effective to mix two solutions. We assume that the folding process is irreversible at low pH values and that the formation of the intramolecular i-motif and the dimers is two parallel reactions. One is a first-order process and the other is a second-order process, respectively:



where  $k_1$ ,  $k_2$  are the rate constants for eqs 5 and 6, respectively. If the concentrations of  $\text{DNA}_{\text{i-motif}}$  and  $(\text{DNA})_2$  are  $x(t)$  and  $y(t)$  at time  $t$ , respectively, and if the initial DNA molar concentration is  $C$ , the differential forms of the rate law are

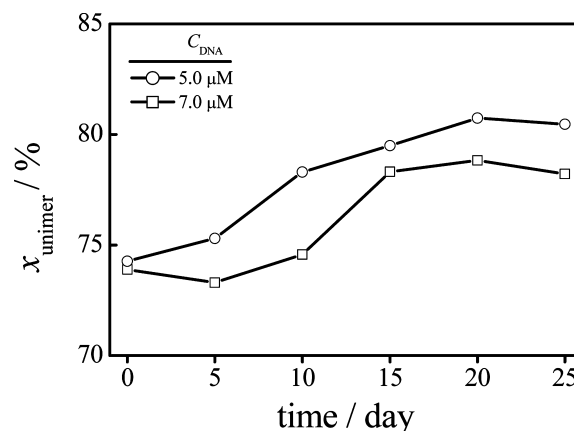
$$\frac{dx(t)}{dt} = k_1(C - x - 2y) \quad (7)$$

$$\frac{dy(t)}{dt} = k_2(C - x - 2y)^2 \quad (8)$$

The initial conditions are that  $x = 0$  and  $y = 0$  when  $t = 0$ . According to Chen et al., the estimated folding rate when the pH jumped from 8.01 to 4.5 was  $\sim 8 \text{ s}^{-1}$  if the formation of dimers does not affect the circular dichroism signal too much.<sup>31</sup> Moreover, as mentioned above, when the DNA concentration is  $2.0 \mu\text{M}$ , the mean collision time  $t_c$  is 0.03 ms and the folding of i-motif DNA finishes in  $\sim 300$  ms; thus, we reasonably set a steric factor  $P$  as  $1 \times 10^4$ , which means that one dimer will form after  $1 \times 10^4$  times of collision. For diffusion-controlled reactions, the rate constant  $k_d = (8k_B T / 3\eta) N_A 10^3 \text{ M}^{-1} \text{ s}^{-1}$  with  $k_B$ ,  $T$ ,  $\eta$ , and  $N_A$  being the Boltzmann constant, the absolute temperature, the viscosity of the solution, and the Avogadro's number. Therefore,  $k_d \sim 6 \times 10^9 \text{ M}^{-1} \text{ s}^{-1}$  at  $20$  °C in aqueous

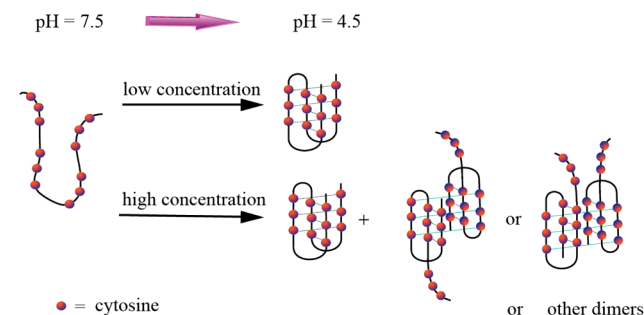
solution. Thus, the second-order rate constant  $k_2 \sim P \times k_d \sim 6 \times 10^5 \text{ M}^{-1} \text{ s}^{-1}$ . On the basis of the  $k_1$  and  $k_2$  values and the initial conditions, we can estimate the final weight percentage of the unimer by MATLAB program (Figure 7). Clearly, it is consistent with our experimental data.

Figure 8 shows the time dependence of the weight percentage of the unimer.  $x_{\text{unimer}}$  increases in the first 15



**Figure 8.** Time dependence of the weight percentage of the unimer ( $x_{\text{unimer}}$ ) of i-motif DNA with different concentrations of  $5.0 \mu\text{M}$  and  $7.0 \mu\text{M}$  at  $20$  °C.

days. After 15 days, the  $x_{\text{unimer}}$  no longer changes with time. The facts indicate that the DNA unimer with an intramolecular i-motif structure is more stable than the dimer at room temperature. The dimers are relatively stable in several days which ensure the reliability of the results from sedimentation velocity experiments. Figure 8 also shows that the change in  $x_{\text{unimer}}$  increased as the initial DNA concentration decreases, indicating that the dimers formed at higher initial DNA concentration is more stable than that formed at lower initial DNA concentration. The possible reason is that the frequency of the collision is higher at higher initial DNA concentration, which means that some dimers with strong interactions may replace the dimers with weak interactions during the collision. Figure 9 schematically summarizes the pH-induced folding



**Figure 9.** Schematic illustration of the initial concentration dependence of the pH-induced folding pathway of the i-motif DNA.

pathway of the i-motif DNA at different concentrations. When the DNA concentration is low, only intramolecular DNA i-motif forms. When the DNA concentration is high, DNA unimer with intramolecular i-motif structure and dimers coexist.

Understanding the conformational change of individual DNA chains and their dimerization is significant for designing DNA-based devices. Yurke et al. designed molecular tweezers made

from three oligonucleotide strands which were different from the DNA i-motif used in our current study.<sup>34</sup> It was found that the formation of dimers can cause the properties of the device to decrease. They proposed that formation of the dimers could be avoided by tethering the tweezers to a solid substrate to prevent the interaction with each other. Alternatively, the dimers could be avoided by lowering the DNA concentration.<sup>9</sup>

The dimerization during the folding is important for the study of pH-induced folding kinetics. To investigate the folding kinetics of individual DNA i-motif chains, the concentration of DNA i-motif in aqueous solutions should be smaller than 1.0  $\mu\text{M}$  to avoid the formation of dimers. As this DNA is a fragment of the vertebrate telomere, the formation of the monomeric and dimeric i-motif structures for this C-rich DNA might be biologically relevant and might bring two homologous chromatids together during meiosis possibly with the help of several nuclear proteins.<sup>4,5,48,49</sup>

## CONCLUSION

In conclusion, we have investigated the pH-induced conformational change of individual i-motif DNA chains by sedimentation velocity analytical ultracentrifugation. At  $\text{pH} < 6$ ,  $R_h$  is nearly a constant, indicating that the DNA adopts an i-motif conformation with a smaller  $R_h$  of  $\sim 1.33$  nm. The sudden increase in  $R_h$  in the pH range 6–7 reflects the conformational change from an i-motif to a random coil. Then,  $R_h$  levels off at  $\text{pH} > 7$ . Moreover, our results show that relatively stable dimers can form as the pH jumped from 7.5 to 4.5. The weight percentage of the dimers increases with the increase in the initial DNA concentration. We believe that the pH-induced conformational change of individual i-motif DNA chains and that the formation of dimers are significant for the development of related DNA-based devices and for understanding the functions of the telomeres containing repeated cytosine-rich sequences.

## AUTHOR INFORMATION

### Corresponding Authors

\*(X.Y.) E-mail: xdy@ustc.edu.cn.

\*(G.Z.) E-mail: msgzzhang@scut.edu.cn.

### Notes

The authors declare no competing financial interest.

## ACKNOWLEDGMENTS

The authors thank Professor Shiyong Liu for generously providing access to the stopped-flow spectroscopy. The financial support of the National Program on Key Basic Research Project (2012CB933800), the National Natural Scientific Foundation of China (NNSFC) Projects (21274140 and 21234003), and the Scientific Research Foundation for the Returned Overseas Chinese Scholars, State Education Ministry, is gratefully acknowledged.

## REFERENCES

- (1) Gehring, K.; Leroy, J. L.; Guéron, M. A Tetrameric DNA Structure with Protonated Cytosine-Cytosine Base Pairs. *Nature* **1993**, *363*, 561–565.
- (2) Chen, L. Q.; Cai, L.; Zhang, X. H.; Rich, A. Crystal Structure of a Four-Stranded Intercalated DNA:d(C<sub>4</sub>). *Biochemistry* **1994**, *33*, 13540–13546.
- (3) Eid, J. E.; Sollner-Webb, B. St-1, a 39-Kilodalton Protein in *Trypanosoma Brucei*, Exhibits a Dual Affinity for the Duplex Form of

the 29-Base-Pair Subtelomeric Repeat and Its C-Rich Strand. *Mol. Cell. Biol.* **1995**, *15*, 389–397.

- (4) Marsich, E.; Piccini, A.; Xodo, L. E.; Manzini, G. Evidence for a HeLa Nuclear Protein That Binds Specifically to the Single-Stranded d(CCCTAA)<sub>n</sub> Telomeric Motif. *Nucleic Acids Res.* **1996**, *24*, 4029–4033.

- (5) Marsich, E.; Xodo, L. E.; Manzini, G. Widespread Presence in Mammals and High Binding Specificity of a Nuclear Protein That Recognises the Single-Stranded Telomeric Motif (CCCTAA)<sub>n</sub>. *Eur. J. Biochem.* **1998**, *258*, 93–99.

- (6) Lacroix, L.; Liénard, H.; Labourier, E.; Djavaheri-Mergny, M.; Lacoste, J.; Leffers, H.; Tazi, J.; Hélène, C.; Mergny, J. L. Identification of Two Human Nuclear Proteins That Recognise the Cytosine-Rich Strand of Human Telomeres in Vitro. *Nucleic Acids Res.* **2000**, *28*, 1564–1575.

- (7) Guéron, M.; Leroy, J. L. The i-Motif in Nucleic Acids. *Curr. Opin. Struct. Biol.* **2000**, *10*, 326–331.

- (8) Cornuel, J. F.; Moraillon, A.; Guéron, M. Participation of Yeast Inosine 5'-Monophosphate Dehydrogenase in an in Vitro Complex with a Fragment of the C-Rich Telomeric Strand. *Biochimie* **2002**, *84*, 279–289.

- (9) Liu, D. S.; Balasubramanian, S. A Proton-Fuelled DNA Nanomachine. *Angew. Chem., Int. Ed.* **2003**, *42*, 5734–5736.

- (10) Seeman, N. C. From Genes to Machines: DNA Nanomechanical Devices. *Trends Biochem. Sci.* **2005**, *30*, 119–125.

- (11) Shu, W. M.; Liu, D. S.; Watari, M.; Riener, C. K.; Strunz, T.; Welland, M. E.; Balasubramanian, S.; McKendry, R. A. DNA Molecular Motor Driven Micromechanical Cantilever Arrays. *J. Am. Chem. Soc.* **2005**, *127*, 17054–17060.

- (12) Liedl, T.; Simmel, F. C. Switching the Conformation of a DNA Molecule with a Chemical Oscillator. *Nano Lett.* **2005**, *5*, 1894–1898.

- (13) Liu, D. S.; Bruckbauer, A.; Abell, C.; Balasubramanian, S.; Kang, D. J.; Klenerman, D.; Zhou, D. J. A Reversible pH-Driven DNA Nanoswitch Array. *J. Am. Chem. Soc.* **2006**, *128*, 2067–2071.

- (14) Bath, J.; Turberfield, A. J. DNA Nanomachines. *Nat. Nanotechnol.* **2007**, *2*, 275–284.

- (15) Liu, H. J.; Xu, Y.; Li, F. Y.; Yang, Y.; Wang, W. X.; Song, Y. L.; Liu, D. S. Light-Driven Conformational Switch of i-Motif DNA. *Angew. Chem., Int. Ed.* **2007**, *46*, 2515–2517.

- (16) Mao, Y. D.; Liu, D. S.; Wang, S. T.; Luo, S. N.; Wang, W. X.; Yang, Y. L.; Ouyang, Q.; Lei, J. Alternating-Electric-Field-Enhanced Reversible Switching of DNA Nanocontainers with pH. *Nucleic Acids Res.* **2007**, *35*, e33.

- (17) Wang, W. X.; Liu, H. J.; Liu, D. S.; Xu, Y. R.; Yang, Y.; Zhou, D. J. Use of the Interparticle i-Motif for the Controlled Assembly of Gold Nanoparticles. *Langmuir* **2007**, *23*, 11956–11959.

- (18) Modi, S.; Swetha, M. G.; Goswami, D.; Gupta, G. D.; Mayor, S.; Krishnan, Y. A DNA Nanomachine That Maps Spatial and Temporal pH Changes inside Living Cells. *Nat. Nanotechnol.* **2009**, *4*, 325–330.

- (19) Topping, T.; Toftegaard, R.; Arnbjerg, J.; Ogilby, P. R.; Gothelf, K. V. Reversible pH-Regulated Control of Photosensitized Singlet Oxygen Production Using a DNA i-Motif. *Angew. Chem., Int. Ed.* **2010**, *49*, 7923–7925.

- (20) He, D. G.; He, X. X.; Wang, K. M.; Cao, J.; Zhao, Y. X. A Photon-Fueled Gate-Like Delivery System Using i-Motif DNA Functionalized Mesoporous Silica Nanoparticles. *Adv. Funct. Mater.* **2012**, *22*, 4704–4710.

- (21) Zhao, Y.; Cao, L.; Ouyang, J.; Wang, M.; Wang, K.; Xia, X. H. Reversible Plasmonic Probe Sensitive for pH in Micro/Nanospaces Based on i-Motif-Modulated Morpholino-Gold Nanoparticle Assembly. *Anal. Chem.* **2013**, *85*, 1053–1057.

- (22) Wang, C. X.; Du, Y.; Wu, Q.; Xuan, S. G.; Zhou, J. J.; Song, J. B.; Shao, F. W.; Duan, H. W. Stimuli-Responsive Plasmonic Core-Satellite Assemblies: i-Motif DNA Linker Enabled Intracellular pH Sensing. *Chem. Commun.* **2013**, *49*, 5739–5741.

- (23) Li, T.; Famulok, M. i-Motif-Programmed Functionalization of DNA Nanocircles. *J. Am. Chem. Soc.* **2013**, *135*, 1593–1599.

- (24) Ahmed, S.; Henderson, E. Formation of Novel Hairpin Structures by Telomeric C-Strand Oligonucleotides. *Nucleic Acids Res.* **1992**, *20*, 507–511.
- (25) Leroy, J. L.; Guéron, M.; Mergny, J. L.; Hélène, C. Intramolecular Folding of a Fragment of the Cytosine-Rich Strand of Telomeric DNA into an i-Motif. *Nucleic Acids Res.* **1994**, *22*, 1600–1606.
- (26) Yang, Y. H.; Sun, Y. W.; Yang, Y.; Xing, Y. Z.; Zhang, T.; Wang, Z. M.; Yang, Z. Q.; Liu, D. S. Influence of Tetra(Ethylene Glycol) (EG<sub>4</sub>) Substitution at the Loop Region on the Intramolecular DNA i-Motif. *Macromolecules* **2012**, *45*, 2643–2647.
- (27) Yang, Y.; Liu, G.; Liu, H. J.; Li, D.; Fan, C. H.; Liu, D. S. An Electrochemically Actuated Reversible DNA Switch. *Nano Lett.* **2010**, *10*, 1393–1397.
- (28) Mergny, J. L. Fluorescence Energy Transfer as a Probe for Tetraplex Formation: The i-Motif. *Biochemistry* **1999**, *38*, 1573–1581.
- (29) Choi, J.; Kim, S.; Tachikawa, T.; Fujitsuka, M.; Majima, T. pH-Induced Intramolecular Folding Dynamics of i-Motif DNA. *J. Am. Chem. Soc.* **2011**, *133*, 16146–16153.
- (30) Zhou, J.; Wei, C. Y.; Jia, G. Q.; Wang, X. L.; Feng, Z. C.; Li, C. Formation of i-Motif Structure at Neutral and Slightly Alkaline pH. *Mol. BioSyst.* **2010**, *6*, 580–586.
- (31) Chen, C.; Li, M.; Xing, Y. Z.; Li, Y. M.; Joedecke, C. C.; Jin, J.; Yang, Z. Q.; Liu, D. S. Study of pH-Induced Folding and Unfolding Kinetics of the DNA i-Motif by Stopped-Flow Circular Dichroism. *Langmuir* **2012**, *28*, 17743–17748.
- (32) Jin, K. S.; Shin, S. R.; Ahn, B.; Rho, Y.; Kim, S. J.; Ree, M. pH-Dependent Structures of an i-Motif DNA in Solution. *J. Phys. Chem. B* **2009**, *113*, 1852–1856.
- (33) Xia, H. W.; Hou, Y.; Ngai, T.; Zhang, G. Z. pH Induced DNA Folding at Interface. *J. Phys. Chem. B* **2010**, *114*, 775–779.
- (34) Yurke, B.; Turberfield, A. J.; Mills, A. P.; Simmel, F. C.; Neumann, J. L. A DNA-Fuelled Molecular Machine Made of DNA. *Nature* **2000**, *406*, 605–608.
- (35) Schuck, P. Size-Distribution Analysis of Macromolecules by Sedimentation Velocity Ultracentrifugation and Lamm Equation Modeling. *Biophys. J.* **2000**, *78*, 1606–1619.
- (36) Lebowitz, J.; Lewis, M. S.; Schuck, P. Modern Analytical Ultracentrifugation in Protein Science: A Tutorial Review. *Protein Sci.* **2002**, *11*, 2067–2079.
- (37) Kaushik, M.; Suehl, N.; Marky, L. A. Calorimetric Unfolding of the Bimolecular and i-Motif Complexes of the Human Telomere Complementary Strand, d(C<sub>3</sub>TA<sub>2</sub>)<sub>4</sub>. *Biophys. Chem.* **2007**, *126*, 154–164.
- (38) Lieblein, A. L.; Buck, J.; Schlepckow, K.; Fürtig, B.; Schwalbe, H. Time-Resolved NMR Spectroscopic Studies of DNA i-Motif Folding Reveal Kinetic Partitioning. *Angew. Chem., Int. Ed.* **2012**, *51*, 250–253.
- (39) Provencher, S. W. A Constrained Regularization Method for Inverting Data Represented by Linear Algebraic or Integral Equations. *Comput. Phys. Commun.* **1982**, *27*, 213–227.
- (40) Provencher, S. W. Contin: a General Purpose Constrained Regularization Program for Inverting Noisy Linear Algebraic and Integral Equations. *Comput. Phys. Commun.* **1982**, *27*, 229–242.
- (41) Cohen, G.; Eisenberg, H. Deoxyribonucleate Solutions: Sedimentation in a Density Gradient Partial Specific Volumes Density and Refractive Index Increments and Preferential Interactions. *Biopolymers* **1968**, *6*, 1077–1100.
- (42) Durchschlag, H. *Specific Volumes of Biological Macromolecules and Some Other Molecules of Biological Interest*. Springer-Verlag: New York, 1986.
- (43) Heeb, M. J.; Schuck, P.; Xu, X. Protein S Multimers and Monomers Each Have Direct Anticoagulant Activity. *J. Thromb. Haemost.* **2006**, *4*, 385–391.
- (44) Fernandez, S.; Eritja, R.; Aviñó, A.; Jaumot, J.; Gargallo, R. Influence of pH, Temperature and the Cationic Porphyrin TMPyP4 on the Stability of the i-Motif Formed by the 5'-(C<sub>3</sub>TA<sub>2</sub>)<sub>4</sub>-3' Sequence of the Human Telomere. *Int. J. Biol. Macromol.* **2011**, *49*, 729–736.
- (45) Alberti, P.; Mergny, J. L. DNA Duplex-Quadruplex Exchange as the Basis for a Nanomolecular Machine. *Proc. Natl. Acad. Sci. U.S.A.* **2003**, *100*, 1569–1573.
- (46) Manzini, G.; Yathindra, N.; Xodo, L. E. Evidence for Intramolecularly Folded i-DNA Structures in Biologically Relevant CCC-Repeat Sequences. *Nucleic Acids Res.* **1994**, *22*, 4634–4640.
- (47) Dailey, M. M.; Miller, M. C.; Bates, P. J.; Lane, A. N.; Trent, J. O. Resolution and Characterization of the Structural Polymorphism of a Single Quadruplex-Forming Sequence. *Nucleic Acids Res.* **2010**, *38*, 4877–4888.
- (48) Phan, A. T.; Guéron, M.; Leroy, J. L. The Solution Structure and Internal Motions of a Fragment of the Cytidine-Rich Strand of the Human Telomere. *J. Mol. Biol.* **2000**, *299*, 123–144.
- (49) Sen, D.; Gilbert, W. Formation of Parallel Four-Stranded Complexes by Guanine-Rich Motifs in DNA and Its Implications for Meiosis. *Nature* **1988**, *334*, 364–366.